ELSEVIER

Journal of Neuroscience Methods 104 (2001) 155–163

JOURNAL OF NEUROSCIENCE METHODS

www.elsevier.com/locate/jneumeth

The neuronal refractory period causes a short-term peak in the autocorrelation function

Izhar Bar-Gad [a,*], Ya'acov Ritov [b], Hagai Bergman [a,c]

[a] *Center for Neural Computation, The Hebrew University, Jerusalem, Israel*
[b] *Department of Statistics, The Hebrew University, Jerusalem, Israel*
[c] *Department of Physiology, The Hebrew University — Hadassah Medical School, Jerusalem, Israel*

Received 4 July 2000; received in revised form 20 September 2000; accepted 22 September 2000

Abstract

Autocorrelation functions are a major tool for the understanding of single-cell firing patterns. Short-term peaks in autocorrelation functions have previously been interpreted as a tendency towards bursting activity or elevated probability to emit spikes in a short time-scale. These peaks can actually be a result of the firing of a neuron with a refractory period followed by a period of constant firing probability. Analytic studies and simulations of such neurons replicate the autocorrelation functions of real-world neurons. The relative size of the peak increases with the refractory period and with the firing rate of the cell. This phenomenon is therefore more notable in areas such as the globus pallidus and cerebellum and less clear in the cerebral cortex. We describe here a compensation factor that can be calculated from the neuron's hazard function. This factor can be removed from the original autocorrelation function to reveal the underlying firing pattern of the cell.

Keywords: Firing pattern; Bursts; Hazard function; Basal ganglia; Globus pallidus

1. Introduction

Spike train analysis – the heart of the analysis in most studies of extracellular recordings – is based on the timing of action potentials, while neglecting subthreshold phenomena and changes in spike shape and amplitude. Computing the autocorrelation function (Perkel et al., 1967a) is a common first step toward revealing a spike train's internal structure. This function describes the probability that a neuron will emit a spike as a function of the time elapsed from another firing of a spike by that neuron.

A prominent feature of all neuronal autocorrelation functions is the refractory period caused by the inability of neurons to emit two spikes in close proximity. Neuronal autocorrelation functions (also known as autocorrelograms) are often categorized as flat, oscillatory or bursty according to the shape of the function following the refractory period (Wilson and Groves, 1981; Munemori et al., 1984; Wichmann et al., 1994). Early simulation studies (Segundo et al., 1968) have demonstrated a continuous spectrum of firing patterns ranging from random (flat autocorrelogram), to early mode types (autocorrelograms with a single short peak), and finally to periodic correlograms. This continuous gradation was achieved simply by changing the number or the pattern of the inputs to the simulated neuron. However, later studies have usually assumed a more discrete classification of the firing patterns of neurons. In the canonical interpretation, flat autocorrelation functions reflect neurons with a constant probability for firing a spike (Abeles, 1982a); oscillatory autocorrelation functions reflect periodic oscillations in the neurons' firing probability (Filion, 1979; Engel et al., 1991; Bergman et al. 1994a); and a peak in the autocorrelation functions reflects the cells' tendency to fire several action potentials in rapid succession, called bursting (Wichmann et al., 1994).

Bursting activity can be caused by intrinsic properties of the neurons, such as elevated calcium or calcium

* Corresponding author. Tel.: +972-2-6757388; fax: +972-2-6439736.
E-mail address: izharb@alice.nc.huji.ac.il (I. Bar-Gad).

0165-0270/01/$ - see front matter
PII: S0165-0270(00)00335-6

conductance levels, or by extrinsic input, such as prolonged synchronous synaptic activity. Bursts may have a special role in synaptic plasticity and information processing in the brain (Lisman, 1997). The definition of bursting activity varies according to the research field. Intracellular/computational researchers use the definition of firing dynamics on multiple time-scales (Rinzel, 1987). Researchers using extracellular recording methods in behaving animals use the functional definition of enhanced firing probability on a short time-scale following the emission of spikes (Abeles, 1982b). The area of the peak in the autocorrelation function is used for estimating the average burst size, that is, the number of spikes within a burst is approximately twice the size of the area (Abeles, 1982b; Bergman et al., 1994a; Colder et al., 1996).

In this manuscript we show that short peaks in the autocorrelation function may be the result of the refractory period of cells with high firing rate and not of the elevated firing probability (bursting activity). We further demonstrate how this effect can be compensated by calculation of an equivalent renewal process using parameters extracted from the hazard function of the cell.

2. Methods

2.1. Electrophysiological data

Electrophysiological examples were obtained from various physiological recordings made previously in our laboratory (Wichmann et al., 1994, 1999; Nini et al., 1995). We used standard physiological techniques for extracellular recording of spiking activity of neurons in behaving primates (Nini et al., 1995). Stability and recording quality were evaluated off-line, and only well-isolated and stable spike trains — those with stable spike waveforms, stable firing rate and consistent responses to behavioral events — were included in this study. The length of the recordings varied in the range of 200–3000 s. The autocorrelation functions were calculated using 1-ms bins and normalized to reflect the firing rate for each bin using standard methods (Abeles, 1982b). The autocorrelation values at time zero (reflecting the number of spikes) were removed.

2.2. Simulation technique

The neurons were modeled as a realization of a renewal process featuring reduced initial probability followed by a constant probability. A renewal process is defined as effected only from the last spike and not from any event prior to it, i.e. all sub-threshold phenomena are being reset by the last action potential. This specific renewal process has been previously addressed as a Poisson process with a refractory period (MacGregor, 1987; Reich et al., 1998). In the model, cells have a constant firing probability (p) for each time bin (Δt). However, after a spike occurs the neuron enters a refractory period (of length τ_r bins) in which its probability of firing is smaller than the steady-state probability. We used two different kinds of refractory periods: a simple refractory period was defined as zero firing probability for the entire period; a complex refractory period was defined by a sequence of probabilities $p_r(1)\ldots p_r(\tau_r)$ with values between 0 and p. The values of p and τ_r depend on the brain area being modeled, e.g., typical values for the globus pallidus are $0.05 \le p \le 0.25$, $4 \text{ ms} \le \tau_r \le 8$ ms (DeLong, 1971). The time bin (Δt) is assumed to be smaller than the refractory period, and the probability of multiple spikes in the same bin is assumed to be very small. Throughout both the electrophysiological recordings and the simulations the default bin size was 1 ms. The length of the simulation was in the range of the duration of the electrophysiological recordings (10^6 bins = 1000 s).

3. Results

3.1. Short-term peaks in electrophysiological studies

Neurons in many areas of the nervous system display short-term 'bursty' autocorrelation functions. Some of the autocorrelation functions of such cells are shown in Fig. 1: a neuron from the globus pallidus external segment (1a) and from the internal segment (1b), a neuron from the substantia nigra pars reticulata (1c) and a subthalamic nucleus neuron (1d). Other examples from the literature include spinothalamic tract neurons in the spinal cord (Surmeier et al., 1989, Figs. 6c and 7c), neurons of the somatosensory cortex (Ahissar and Vaadia, 1990, Figs. 2 and 3), striatum (Wilson 1993, Fig. 13b,c), substantia nigra (Wilson et al., 1977, Figs. 1 and 8), and cerebellum (Ebner and Bloedel, 1981, Fig. 2c). The shape of the autocorrelation is characterized by a generally flat function except for a short-term structure at time-scales of several milliseconds up to a few tens of milliseconds. These autocorrelation graphs can be clearly divided into several consecutive phases (1a). The refractory phase consists of the refractory period of the neuron and features low correlation values. This phase is followed by an elevated correlation phase featuring a peak in the correlation values. After this phase the autocorrelation function returns to a steady-state value, sometimes with a short, damped oscillation phase (for example, 1c and see Bergman et al., 1994b, Fig. 2d; Ebner and Bloedel, 1981, Fig. 2d). Traditionally (Rodieck et al., 1962; Perkel et al., 1967a; Abeles, 1982b), cells with such autocorrelation graphs were viewed as neurons with a tendency for burst

creation due to the peak in the autocorrelation. However, our new analysis and simulations will show that such a graph can arise from the activity of a cell that does not change its firing probability following previous activity.

3.2. Simple refractory period model — simulation and analysis

The simple refractory period (SRP) model describes a cell with an absolute refractory period but no relative refractory period. This simplified model can be solved analytically in a simple manner, and the logic of its results is easily explained. We simulated the SRP model by setting firing probability (p) as a function of time elapsed since the last spike (t). This probability is actually the hazard function of the simulated neuron, the probability of a spike at time t assuming that no spikes were emitted during the interval $0 \rightarrow t-1$:

$$p_t = \begin{cases} 0 & t \le \tau_r \\ p & t > \tau_r \end{cases} \quad (1)$$

The result of simulating such a neuron for the SRP model is shown (2a), and the resemblance to the 'bursty' autocorrelation functions is readily apparent. The shape of the autocorrelation function clearly resembles the experimental results, with typical short-term periods of refractory phase, elevated phase and damping oscillations leading to steady state.

The exact values of the autocorrelation function can be calculated analytically for the SRP model. The value of the function at offset (time) t can be described by the correlation variables a_t (reflecting the firing rate λ_t multiplied by the bin size Δt). The value of the correlation variable during the refractory period is zero since the probability of firing is zero. The correlation value after that period depends on the probability that a spike occurred during the previous τ_r bins, but is otherwise independent of all prior events.

$$a_t = \begin{cases} 0 & t \le \tau_r \\ \left(1 - \sum_{i=1}^{\tau_r} a_{t-i}\right) & t > \tau_r \end{cases} \quad (2)$$

This function reaches maximum at the bin immediately following the refractory period (offset $\tau_r + 1$), and its value is

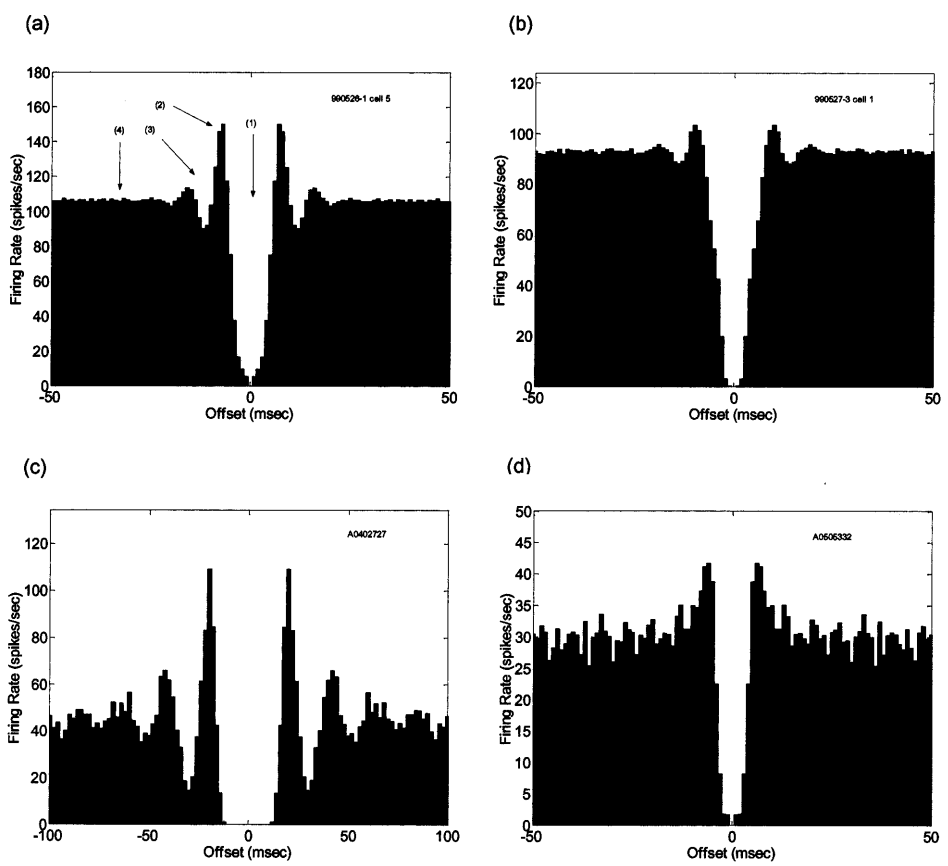

Fig. 1. Examples of autocorrelation functions: (a) globus pallidus external segment (GPe); (b) globus pallidus internal segment (GPi); (c) substantia nigra pars reticulata (SNr); (d) subthalamic nucleus (STN). Phases in the autocorrelation function: (1) refractory phase; (2) elevated phase; (3) oscillatory phase; (4) steady state.

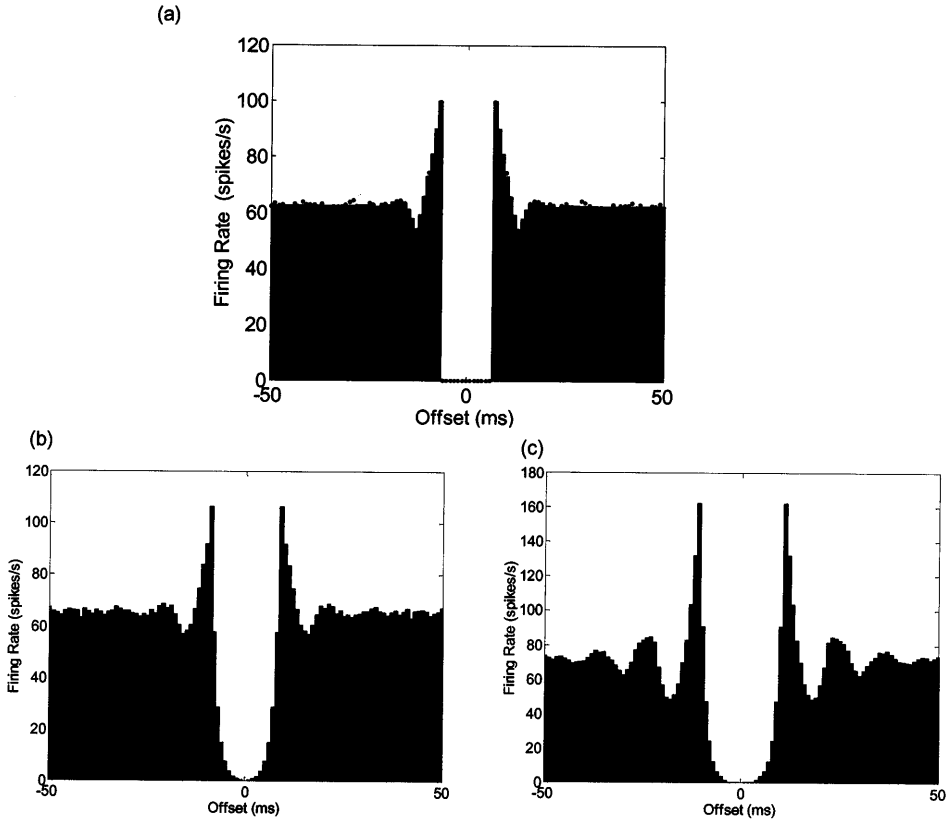

Fig. 2. Simulated and analytically calculated autocorrelation functions displaying short-term peaks. (a) Simple refractory period ($\tau_r = 6$ ms, $P = 0.1$), solid bars represent the analytically calculated value and the dots represent the simulated neuron. The peak in the graph is at time $\tau_r + 1 \rightarrow 7$ ms, $\lambda_{\tau_r+1} = p/\Delta t \rightarrow 100$ spikes/s. The steady state of the graph is $\lambda_\infty = p/[\Delta t \cdot (1 + p \cdot \tau_r)] \rightarrow 62.5$ spikes/s. (b) Simulated neuron using complex refractory period ($\tau_r = 8$ ms, $p = 0.12$). (c) Simulated neuron using complex refractory ($\tau_r = 10$ ms, $p = 0.25$). Both complex cases use exponential refractory periods ($p_t = k^{(\tau_r + 1 - t)} \cdot p \quad t \leq \tau_r$, $k = 0.5$).

$$a_{\tau_r+1} = p \tag{3}$$

The limit of the process at infinity satisfies

$$a_\infty = (1 - \tau_r a_\infty) \cdot p \quad t \rightarrow \infty \tag{4}$$

leading to the steady-state value

$$a_\infty = \frac{p}{1 + p \cdot \tau_r} \tag{5}$$

An example of an analytically calculated autocorrelation function is shown (2a), and a qualitative explanation for the results appears in Section 4.

3.3. Complex refractory period model — simulation and analysis

The complex refractory period (CRP) model describes a cell with a refractory period containing firing probabilities smaller than the steady-state probability. In most cases, there would be an absolute refractory period followed by a period of monotonically increasing probability, but the analysis is not limited to such cases. The cells were simulated using the general description of the firing probability (hazard function):

$$\begin{aligned} p_t &< p \quad t \leq \tau_r \\ p_t &= p \quad t > \tau_r \end{aligned} \tag{6}$$

Calculating the size of the autocorrelation function at time t requires definition of the parameter q_t that reflects the probability for a first spike at offset t, reflecting the inter-spike interval (ISI) distribution. This parameter can either be extracted directly from the ISI distribution or calculated from the hazard function:

$$q_t = p_t \prod_{i=1}^{t-1} (1 - p_i) = p_t \cdot \left(1 - \sum_{i=1}^{t-1} q_i\right) \tag{7}$$

The autocorrelation value at offset t can be calculated recursively:

$$a_t = q_t + \sum_{i=1}^{t-1} q_i a_{t-i} \tag{8}$$

The steady-state value can be calculated from the mean time until the first spike:

$$a_\infty = \frac{1}{\sum_{t=1}^{\infty} q_t \cdot t} \tag{9}$$

The shape and size of the peak in the autocorrelation function are determined by the shape and length of the refractory period as well as by the firing probability (2b, c).

3.4. Quantitative description of the peak phenomenon

The difference between the peak value and the autocorrelation steady-state value (delta peak) varies greatly, depending on various parameters characterizing the neuron. These parameters include the probability of firing, length of the refractory period, and the shape of the refractory function. For simplicity, only the SRP model is analyzed, and some computational results are given for other cases. The delta peak can be estimated by the difference between the peak immediately following the refractory period ($a_{\tau+1}$) and the steady state (a_∞). This delta peak is a function of the duration of the refractory period (τ_r) and firing probability (p), or alternatively the more easily measured average firing rate ($\lambda_\infty = a_\infty/\Delta t$)

$$\Delta a = a_{\tau_r+1} - a_\infty = \frac{p}{\frac{1}{p\cdot\tau_r}+1} = \frac{a_\infty}{\frac{1}{a_\infty\cdot\tau_r}-1} = \frac{\lambda_\infty\Delta t}{\frac{1}{\lambda_\infty\Delta t\cdot\tau_r}-1} \quad (10)$$

The difference increases monotonically with the firing rate λ_∞ and p and is shown in 3a. Complex refractory periods retain the same basic dependency of the phenomenon size on both τ_r and p (or λ_∞). However, the actual size of the difference is generally smaller and depends on the values of the refractory function: $p_r(1)\ldots p_r(\tau_r)$ (3b). The values of calculated differences for parameters typical to different brain areas are shown in Table 1.

The duration of the elevated phase is τ_r but at the end of this phase it may decrease to sub-steady-state values. In cases of very high firing rate or very long refractory periods the autocorrelation function may assume a damped oscillation shape with oscillations of length τ_r (2c). This oscillatory autocorrelation function is the extreme case of this phenomenon, and reflects the fact that neurons with both high firing rates and long refractory periods tend to display periodic discharge patterns. The repetitive discharge of spinal motor neurons is a classical example of this effect. Simulation of the spinal motor neuron firing clearly demonstrates the regularizing effect of the refractory period on the firing pattern of the cell (Kernell, 1968).

3.5. Peak phenomenon estimation and removal from real data

Estimation and removal of the phenomenon from the data can be performed assuming that the neuronal firing may be described as a renewal process. The original autocorrelation function is calculated for the recorded data (4a, b). The first stage consists of assessing the refractory period (length and relative values) and the mean firing probability during the steady state (following the refractory period). These variables can be extracted from the hazard function (h_t) calculated for the neuron (4c, d). Once the mean steady-state value of the hazard function ($\bar{h}$) is calculated, the length of the refractory period is calculated as the number of bins following the reference spike with lower firing probabil-

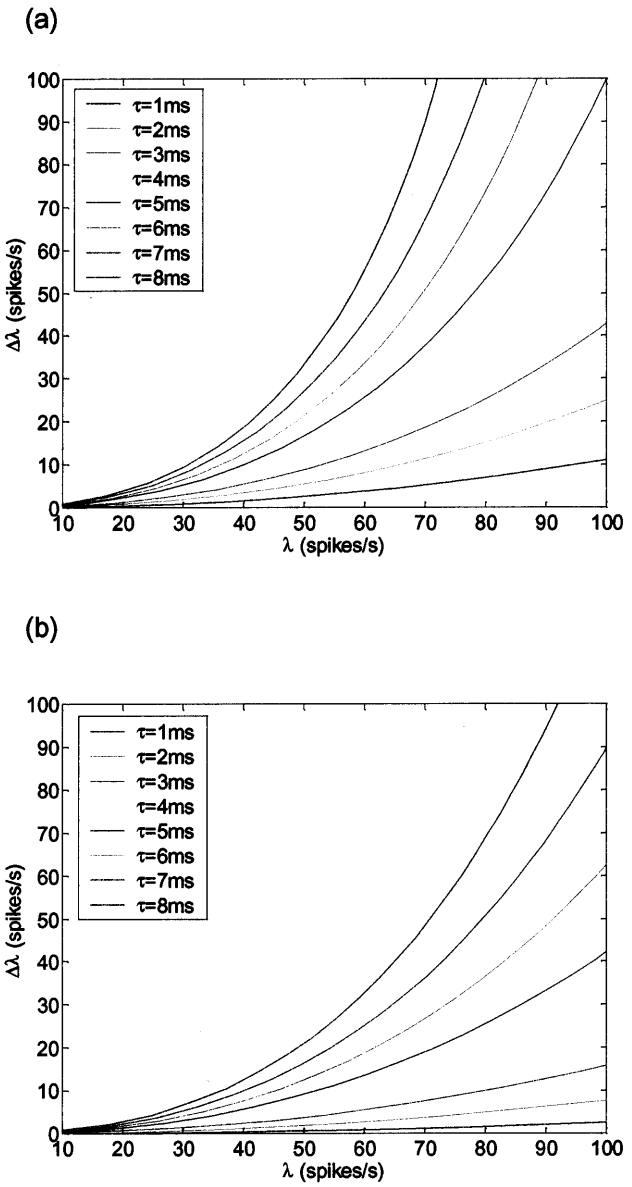

Fig. 3. Quantitative estimation of the amplitude of the short-term peak effect. (a) Estimation of the difference between the maximal peak and the steady state value (delta peak) as a function of the refractory period length (τ_r) and the firing rate (λ) for the SRP model. (b) Estimation of the delta peak for the CRP model using a moderate slope exponential period ($p_t = k^{(\tau_r+1-t)}p \quad t \le \tau_r,\ k = 0.5$).

Table 1
Typical delta peak values in various brain areas[a]

	λ_∞ (Hz)	τ_r (ms)	SRP		CRP	
			$\Delta\lambda$ (Hz)	$\Delta\lambda$ (% of λ_∞)	$\Delta\lambda$ (Hz)	$\Delta\lambda$ (% of λ_∞)
Globus pallidus	60	6	33.75	56.25	18.86	31.43
STN	25	4	2.78	11.11	1.51	6.04
Cortex	5	2	0.05	1.01	0.02	0.40

[a] Typical values of firing rate and refractory period for different brain areas and the expected size of the peak over the steady state assuming SRP and CRP with an exponential shape ($k = 0.5$).

ity and the values of the relative refractoriness can be extracted for that period. The probability of firing following the refractory period is set to the mean value to retain the original firing pattern after the compensation.

$$p_t = \begin{cases} h_t & t \le \tau_r \\ \bar{h} & t > \tau_r \end{cases} \quad (11)$$

The extracted variables enable the construction of a simulated neuron and calculation of its autocorrelation function using and (4e, f). The deviation of the autocorrelation function of the surrogate neuron from its steady state after the refractory period can be removed from the autocorrelation function of the recorded neuron to receive the compensated autocorrelation function (4g, h). The compensation process shows that one of the cells has no underlying bursting activity (4g), whereas the other cell has a significant tendency for bursting (4h).

4. Discussion

The major points emphasized in this article are:

- Short-term peaks in the autocorrelation function do not necessarily reflect bursting activity of the neuron.
- The peaks are significant in neurons featuring high firing rates and/or long refractory periods.
- The underlying firing pattern can be revealed by the compensation method described above.

4.1. Insight into the peak phenomenon

The logic in the seemingly surprising shape of the autocorrelation function derives from understanding the role of the refractory period in shaping the cell's temporal firing pattern. The logic is simple when considering the SRP model: At the end of the refractory period the cell has a probability p for firing. However, at long offsets the probability of firing is influenced by additional refractory periods. This causes the firing probability to decrease to the steady state value $p/(1 + p \cdot \tau_r)$. The logic for the general CRP model is the same; however, the exact values of the peak and steady-state correlations are much less intuitive although they can be formulated nevertheless.

4.2. Real-life applications of the peak phenomenon

Despite the widespread use of autocorrelation, previous studies have not taken the peak phenomenon into account. The main reason for this is that most of the spike train analyses are performed on data collected in areas with low firing rates, such as the cerebral cortex. In these areas the size of the phenomenon is generally very small (Table 1 and Fig. 3). However, in areas with high firing rate, such as the basal ganglia and the cerebellum, the effect is significant and might obscure underlying firing patterns. Moreover, manipulations causing a change in rate (for example lesion or pharmacological treatment) cause a change in the size of the phenomenon that might be interpreted as an effect on the structure of the spike train (Bergman et al., 1994a), instead of being properly interpreted as an epiphenomenon of rate changes. Multi-unit recordings are also characterized by relatively high firing rates. However, the phenomenon will be significantly smaller since the refractory period is only weakly expressed in these recordings. Event related changes in the firing rate of neurons may result in 'burst-like' activity of these neurons. In those cases, methods like PST and shift predictors (Perkel et al., 1967b; Aertsen et al., 1989), or joint interval histograms (Ebner and Bloedel, 1981; Eggermont, 1990) should be applied to compensate first for the event related changes in the firing pattern of the cells.

Many cells in the central nervous system do not fire in a manner which resembles a Poisson process with a refractory period. Instead, they have long-term complex changes in firing probability. However, even these cells are prone to being biased by the effect shown. Therefore, whenever the autocorrelation function displays excessive peaks on short time-scales (up to $2\tau_r$), they must either be compensated or checked by other means for assessing temporal patterns.

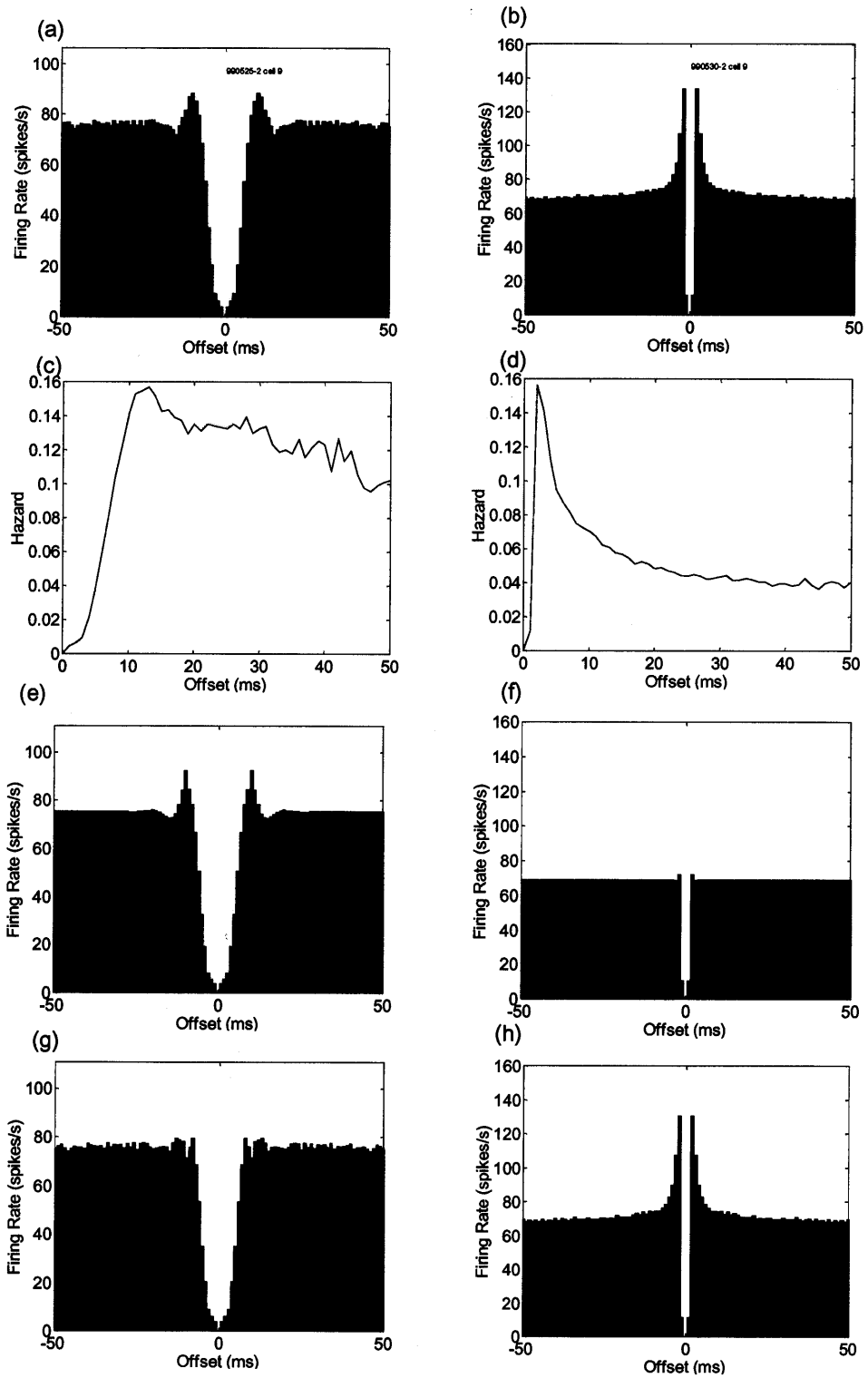

Fig. 4. Estimation and compensation of the short-term peak in the autocorrelation function. (a, b) Measured autocorrelation functions (globus pallidus). (c, d) Estimation of the refractory period length (τ_r) and the mean firing probability ($\bar{h}$) from the hazard functions (h_t). (e, f) Surrogate neurons auto-correlation functions. (g, h) Compensated auto-correlation functions, revealing that one of the cells has an underlying bursting tendency while the other has no such tendency.

4.3. Other methods for analysis of firing pattern of single spike train

For correct estimation of bursting activity of neurons, other methods can be used in conjunction with the compensated autocorrelation function. Several measures use standard mathematical methods such as hazard function calculation (Cox and Lewis, 1966) or inter-spike interval (ISI) estimation (Perkel et al., 1967a) to identify multiple peaks in firing. In addition, comparison of successive self-convolutions of the ISI (an order-independent version of the autocorrelation function) can be made with the autocorrelation function. A mismatch between the order-independent and the actual autocorrelation functions indicates a higher order dependence that might be caused by bursting activity (MacGregor and Lewis, 1977). However, these methods fail to reflect long-term effects in the firing pattern due to small spike counts in bins with long offsets. In addition to these standard measures, specific algorithms have been suggested for burst detection (Legendy and Salcman, 1985; Cocatre-Zilgien and Delcomyn, 1992; Mehta and Bergman, 1995). Only a combination of these methods, with a clear understanding of their limitations, can enable complete understanding of the characteristics of neuronal firing.

Acknowledgements

This study was supported in part by the Israeli Academy of Science, AFIRST and the US–Israel Binational Science Foundation. We thank Moshe Abeles, Opher Donchin and Genela Morris for their critical reading and helpful suggestions. We thank Thomas Wichmann, Gali Havazelet-Heimer, Joshua A. Goldberg and Sharon Maraton for sharing their data with us.

References

Abeles M. Local Cortical Circuits. Berlin: Springer-Verlag, 1982a.

Abeles M. Quantification, smoothing and confidence limits for single-units' histograms. J Neurosci Methods 1982b;5:317–25.

Aertsen AM, Gerstein GL, Habib MK, Palm G. Dynamics of neuronal firing correlation: modulation of "effective connectivity". J Neurophysiol 1989;61:900–17.

Ahissar E, Vaadia E. Oscillatory activity of single units in a somatosensory cortex of an awake monkey and their possible role in texture analysis. Proc Natl Acad Sci USA 1990;87:8935–9.

Bergman H, Wichmann T, Karmon B, DeLong MR. The primate subthalamic nucleus. II. Neuronal activity in the MPTP model of parkinsonism. J Neurophysiol 1994a;72:507–20.

Bergman H, Wichmann T, Karmon B, DeLong MR. Parkinsonian tremor is associated with low frequency neuronal oscillations in selective loops of the basal ganglia. In: Percheron G, McKenzie JS, Feger J, editors. The basal ganglia IV: new ideas and data on structure and function. New York: Plenum Press, 1994b:317–25.

Cocatre-Zilgien JH, Delcomyn F. Identification of bursts in spike trains. J Neurosci Methods 1992;41:19–30.

Colder BW, Frysinger RC, Wilson CL, Harper RM, Engel J. Decreased neuronal burst discharge near site of seizure onset in epileptic human temporal lobes. Epilepsia 1996;37:113–21.

Cox DR, Lewis PAW. The statistical analysis of series of events. London: Metheun & Co Ltd, 1966:1966.

DeLong MR. Activity of pallidal neurons during movement. J Neurophysiol 1971;34:414–27.

Ebner TJ, Bloedel JR. Temporal patterning in simple spike discharge of purkinje cells and its relationship to climbing fiber activity. J Neurophys 1981;45:933–47.

Eggermont JJ. The correlative brain. Theory and experiment in neuronal interaction. Berlin: Springer-Verlag, 1990.

Engel AK, Kreiter AK, Konig P, Singer W. Synchronization of oscillatory neuronal responses between striate and extrastriate visual cortical areas of the cat. Proc Natl Acad Sci USA 1991;88:6048–52.

Filion M. Effects of interruption of the nigrostriatal pathway and of dopaminergic agents on the spontaneous activity of globus pallidus neurons in the awake monkey. Brain Res 1979;178:425–41.

Kernell D. The repetitive impulse discharge of a simple neurone model compared to that of spinal motoneurones. Brain Res 1968;11:685–7.

Legendy CR, Salcman M. Bursts and recurrences of bursts in the spike trains of spontaneously active striate cortex neuron. J Neurophysiol 1985;53:926–39.

Lisman JE. Bursts as a unit of neural information: making unreliable synapses reliable. Trends Neurosci 1997;20:38–43.

MacGregor RJ. Neural and brain modeling. San-Diego: Academic Press Inc., 1987.

MacGregor RJ, Lewis ER. Neural modeling. New York: Plenum Press, 1977.

Mehta MR, Bergman H. Loss of frequencies in autocorrelations and a procedure to recover them. J Neurosci Methods 1995;62:65–71.

Munemori J, Hara K, Kimura M, Sato R. Statistical features of impulse trains in cat's lateral geniculate neurons. Biol Cybern 1984;50:167–72.

Nini A, Feingold A, Slovin H, Bergman H. Neurons in the globus pallidus do not show correlated activity in the normal monkey, but phase-locked oscillations appear in the MPTP model of parkinsonism. J Neurophysiol 1995;74:1800–5.

Perkel DH, Gerstein GL, Moore GP. Neuronal spike trains and stochastic point processes. I. The single spike train. Biophys J 1967a;7:391–418.

Perkel DH, Gerstein GL, Moore GP. Neuronal spike trains and stochastic point processes. II. Simultaneous spike trains. Biophys J 1967b;7:419–40.

Reich DS, Victor JD, Knight BW. The power ratio and the interval map: spiking models and extracellular recordings. J Neurosci 1998;18:10090–104.

Rinzel J. A formal classification of bursting mechanisms in excitable systems. In: Lecture notes in biomathematics, 1987:267–81.

Rodieck RW, Kiang NYS, Gerstein GL. Some quantitative methods for the study of spontaneous activity of single neurons. Biophys J 1962;2:351–68.

Segundo JP, Perkel DH, Wyman H, Hegstad H, Moore GP. Input-output relations in computer-simulated nerve cells. Influence of the statistical properties, strength, number and inter-dependence of excitatory pre-synaptic terminals. Kybernetik 1968;4:157–71.

Surmeier DJ, Honda CN, Willis WD. Patterns of spontaneous discharge in primate spinothalamic neurons. J Neurophysiol 1989;61:106–15.

Wichmann T, Bergman H, DeLong MR. The primate subthalamic nucleus. I. Functional properties in intact animals. J Neurophysiol 1994;72:494–506.

Wichmann T, Bergman H, Starr PA, Subramanian T, Watts RL, DeLong MR. Comparison of MPTP-induced changes in spontaneous neuronal discharge in the internal pallidal segment and in the substantia nigra pars reticulata in primates. Exp Brain Res 1999;125:397–409.

Wilson CJ. The generation of natural firing patterns in neostriatal neurons. Prog Brain Res 1993;99:277–97.

Wilson CJ, Groves PM. Spontaneous firing patterns of identified spiny neurons in the rat neostriatum. Brain Res 1981;220:67–80.

Wilson CJ, Young SJ, Groves PM. Statistical properties of neuronal spike trains in the substantia nigra: cell types and their interactions. Brain Res 1977;136:243–60.